ORIGINAL PAPER

A molecular dynamics study on sI hydrogen hydrate

S. Mondal · S. Ghosh · P. K. Chattaraj

Abstract A molecular dynamics simulation is carried out to explore the possibility of using sI clathrate hydrate as hydrogen storage material. Metastable hydrogen hydrate structures are generated using the LAMMPS software. Different binding energies and radial distribution functions provide important insights into the behavior of the various types of hydrogen and oxygen atoms present in the system. Clathrate hydrate cages become more stable in the presence of guest molecules like hydrogen.

Keywords Binding energy · Hydrogen · MD simulation · Radial distribution function · Structure I (sI) clathrate

Introduction

Hydrogen is the most abundant element in the universe and is the basic building block as well as fuel for stars. It is an essential raw material in innumerable biological and chemical processes. The possibility of use of hydrogen as a fuel has been rigorously analyzed since the early 1970s when the petroleum prices rose sharply. Apart from the eventual scarcity of fossil fuels, when hydrogen burns it produces water rather than greenhouse gases such as CO_2. New challenges impeding hydrogen-use development are not only related to

the efficient production of hydrogen but also related to the development of hydrogen storage technologies. The following requirements are essential for a hydrogen storage medium: (a) feasibility of synthesis at moderate temperature and pressure, (b) moderate temperature and pressure of storage, (c) high energy content per unit mass, (d) high gravimetric weight percent of storage, (e) easy release of hydrogen, and (f) environment friendly by-products [1].

Though clathrate hydrates have a long history of research of approximately 200 years they have received much attention during the last few decades. In 1811 Davy first reported to the Royal Society of Chemistry, London, that a compound of chlorine and water has a higher melting point than that of ice [2]. In 1823 Faraday measured the composition of the compound reported by Davy to be $Cl_2*(H_2O)_{10}$ [3], but no one had reported anything about the structural integrity of the compound. After that with a long silence of almost 128 years, in the early 1950s the sI and structure II (sII) clathrate cages were identified and characterized [4–6]. It is found that the hydrogen clathrates can encage up to 15.6 mass percentage of molecular hydrogen which is significantly above the target of DOE [1, 7–9]. During liberation of hydrogen these clathrates produce water as the only by-product. Thus with all these aspects we can say that clathrate hydrates are not only attractive but also inexpensive hydrogen storage material [1, 8–21].

Previously it was believed that formation of clathrate hydrates was not possible with molecular hydrogen as a guest [19]. However, Mao et al. synthesized and characterized a hydrogen clathrate with the sII structure from a liquid at a pressure of 200 MPa and a temperature of 249 K [6]. One important drawback of the hydrogen clathrate is that there is no accurate determination of number and position of the encaged H_2 molecules inside the clathrate cage at different temperature and pressure. Though there are a large number of theoretical and experimental studies on this most reports are still conflicting [17, 20–24]. Clathrate hydrates are inclusion compounds of host water molecules and nonreactive, small

S. Mondal · P. K. Chattaraj (✉)
Department of Chemistry and Center for Theoretical Studies,
Indian Institute of Technology,
Kharagpur 721302, India
e-mail: pkc@chem.iitkgp.ernet.in

S. Ghosh (✉)
Department of Metallurgical & Materials Engineering,
Indian Institute of Technology,
Kharagpur 721302, India
e-mail: sudipto@metal.iitkgp.ernet.in

Table 1 Lennard-Jones interaction parameters and atomic charges for SPC/E water and the spherical H_2 molecule

Atom	σ_{ij} (Å)	ε_{ij} (kcal/mol)	q (e)
O	3.166	0.1553	−0.8476
H (water)	0.0	0.0	0.4238
H (guest)	3.140	0.0190	0.0

guest molecules. The host cage is formed by H-bonded water molecules [25]. Among three different types of cage structures: sI, sII, and hexagonal cubic structure (sH); which one will be formed is governed by the size and nature of the guest molecules [11, 26–28]. The guest molecules are trapped inside the hydrogen bonded network of water molecules through weak, nonspecific van der Walls interaction as well as in a non-stoichiometric ratio. Among the above mentioned three different types of cage structures, the most common naturally occurring clathrate is sI which contains 46 water molecules that form two pentagonal dodecahedron (5^{12}) and six hexagonal truncated trapezohedron ($5^{12}6^2$) cages in a unit cell [29]. An sI clathrate hydrate can encapsulate small guest molecules of 0.40–0.55 nm size [30]. Jacobson et al. have shown how the size of guest molecules monitor the fate of the structural integrity of clathrate hydrates [31]. From the solid–liquid coexistence curve of sI methane hydrate using different water models in the 0–5000 bar pressure range, Smirnov et al. have shown how the decay temperature decreases with the decrease of cage occupancy [32]. The thermo-physical and structural properties of sI clathrate hydrates are mainly influenced by the host-guest asymmetries [33].

In this work we study the structure and stability of type sI hydrogen hydrate with different number of hydrogen molecules. Our primary target of this work is an attempt toward the advancement of hydrogen storage technologies by exploring sI clathrate hydrates where hydrogen is the only guest molecule.

Computational techniques

We have used LAMMPS package [34] to perform all the molecular dynamics simulations. To model the structure of hydrates with different number of hydrogen molecules we have employed the extended SPC water model [35, 36]. For the entire simulation, instead of hydrogen molecule we have incorporated an imaginary sphere without any atomic charge which resembles hydrogen molecule [37].

The potential energy equation between two atoms i and j can be written as:

$$V_{ij} = \sum_{m \in i} \sum_{n \in j} \frac{q_m q_n}{r_{mn}} + 4\varepsilon_{ij}\left[\left(\frac{\sigma_{ij}}{r_{ij}}\right)^{12} - \left(\frac{\sigma_{ij}}{r_{ij}}\right)^6\right], \qquad (1)$$

where q_m and q_n are the charges on atoms i and j respectively, r_{mn} is the distance between the q_m and q_n charged ith and jth atom, ε_{ij}, σ_{ij} are Lennard-Jones parameters and r_{ij} is the distance between the two interacting atoms i and j.

Interaction potentials of all the above mentioned atoms are given in Table 1.

Interaction potential of unlike atoms has been calculated by using the Lorentz-Berthelot rule [38, 39].

We have taken an orthogonal box of size 68 Å×68 Å× 68 Å, which contains a total of 9936 water molecules. The coordinates of oxygen atoms are mimicked with the coarse grained model of Jacobson et al. [40]. For all the cases we have used periodic boundary conditions and all interatomic interactions in the simulation box are calculated within a cutoff distance of 10.0 Å. The simulation is carried out with a time step of 1.0 fs and equations of motion are integrated with velocity Verlet algorithm [41]. Temperature and pressure scaling are done with the Nose-Hoover thermostat and barostat as employed in the LAMMPS package. The fix shake algorithm is used to freeze the bond length and bond angle of water molecules. A PPPM solver is used with a precision of

Fig. 1 a Optimized structure of empty sI clathrate hydrate, **b** Ruptured structure of empty sI clathrate hydrate during temperature ramping
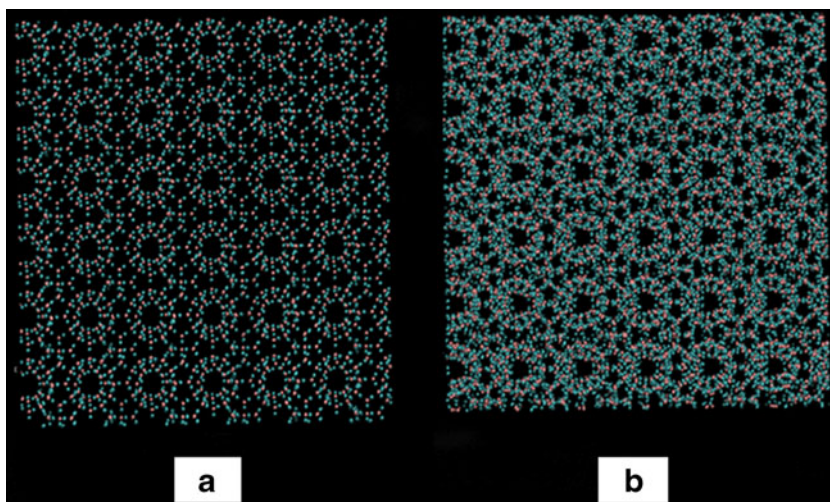
1×10^{-4} to calculate the long-range Coulombic interactions. During energy minimization and temperature ramping the neighbor lists are updated at every time step but for equilibration at every 10 steps. Both NPT and NVT ensembles are employed during temperature and pressure scaling. After the completion of each simulation run (temperature ramping or equilibration) we have checked the lattice constant of the simulated cell and only those are considered where the lattice constants are in the same ratio with the initial one.

We have done simulation with different number of hydrogen molecules. To simulate the empty clathrate cage first we freeze the oxygen coordinates and then energy minimization in this frozen condition leads to the proper alignment of all the water hydrogens to construct the sI clathrate hydrate. We have tried to ramp the temperature of the empty cage but every attempt leads to a rupture of the cage. Structures corresponding to the energy minimized empty cage, as well as the above mentioned ruptured cage are shown in Fig. 1. Figures 1 and 2 are obtained from visual molecular dynamics (VMD) [42] program package.

Thus, the obtained 6×6×6 sI empty clathrate is loaded with three different numbers of hydrogen molecules. All the hydrogen spheres are loaded in $5^{12}6^2$ units in the hydrate slab in a symmetric way (Fig. 2). First we have added 216 hydrogen spheres in the hydrate slab at alternate $5^{12}6^2$ channels of each unit cell. Next 432 hydrogen spheres are added in the same symmetric way maintaining a maximum distance with the previously added hydrogen spheres.

Results and discussion

We have modeled the hydrogen hydrate with 216 hydrogen spheres and the loaded hydrogen goes into each $5^{12}6^2$ cage of each unit cell which is 16.66 % occupation among the total number of $5^{12}6^2$ cages in the clathrate slab. Occupation of 16.66 % of the $5^{12}6^2$ cage thereby resulted in an increase
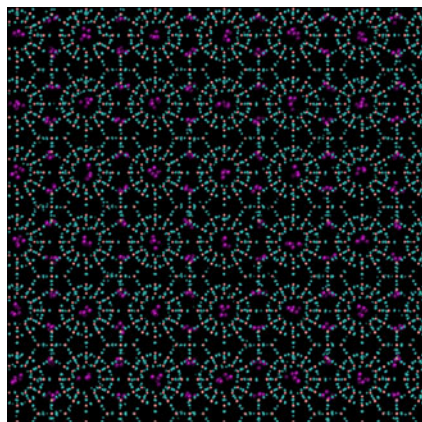
Table 2 Binding energy per hydrogen sphere for the loading of n hydrogen spheres in the $5^{12}6^2$ channel of sI clathrate slab

% Occupied	No. of H_2 molecules (n)	$\Delta E/n$ (kcal/mol)
16.66	216	–3.82
50	648	–4.00

in the volume of the clathrate slab. Addition of further hydrogen sphere in the hydrogen hydrate model takes place in the same way as explained above. Obtained hydrogen hydrates are then equilibrated at 150 K and 100 atm pressure with N-P-T simulation. It is observed that the hydrogen hydrates are stable up to ~200 fs. Binding energies per hydrogen sphere are given in Table 2, which are calculated by using the following equation [27]:

$$sI(0\ H_2) + nH_2 \rightarrow sI(n\ H_2)$$
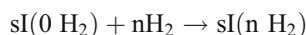
$$\Delta E/n = 1/n\{E[sI(n\ H_2)] - E[sI(0\ H_2)] - 5nRT/2\},$$

where $\Delta E/n$ is the binding energy for loading of each hydrogen molecule, $E[sI(n\ H_2)]$ and $E[sI(0\ H_2)]$ are the energies of n number of hydrogen loaded hydrogen hydrate and of empty clathrate slab respectively. Energy of the hydrogen sphere is $5RT/2$ per mole.

As the $5^{12}6^2$ unit cages are loaded with hydrogen the stability of the system increases and the hydrogen hydrate becomes metastable. Thus we can say that the sI hydrogen hydrate is stable up to a certain extent whereas the empty clathrate cage is unstable.

The radial distribution functions (RDF) [43] of oxygen-oxygen (water) (O-O), hydrogen (water)-hydrogen (water) (H-H^w), oxygen (water)- hydrogen (water) (O-H^w), oxygen (water)-hydrogen (guest) (O-H^g) and hydrogen (water)- hydrogen (guest) (H^w-H^g) for 150 K and 100 atm are studied.

Fig. 2 Metastable structure of the sI hydrogen hydrate which contains a total of 648 H_2 molecules placed in the $5^{12}6^2$ channels
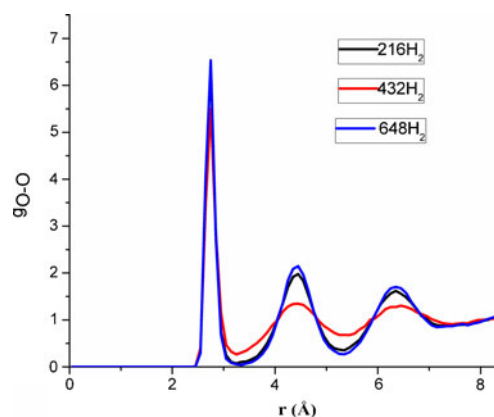

Fig. 3 The O-O radial distribution functions for multiply occupied cages. *Black line* indicates the 216 H_2 molecule encapsulated sI hydrogen hydrate whereas *red* and *blue* indicates those with 432 and 648 H_2 molecules
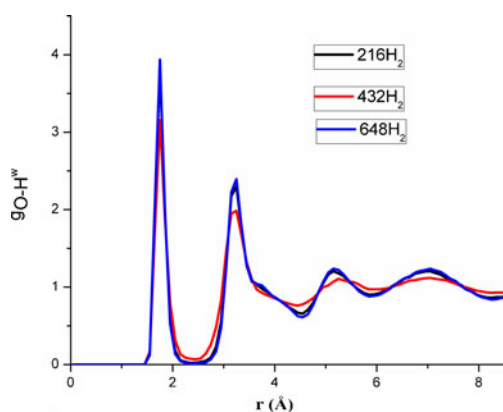
Fig. 4 The O-H (water) radial distribution functions for multiply occupied cages. *Black line* indicates the 216 H_2 molecule encapsulated sI hydrogen hydrate whereas *red* and *blue* indicates those with 432 and 648 H_2 molecules respectively

The RDF of O-O, O-H^w and H-H^w of three different hydrogen loaded hydrogen hydrates are given in Figs. 3, 4 and 5 respectively. Analysis of RDF of O-O of all the hydrogen loaded hydrates (Fig. 3) indicates the first peak at 2.8 Å which mimics the bulk-like structure of water [44] in the presence of a hydrophobic solute, hydrogen. Again from the same figure comparing the second and third peaks of the three hydrogen loaded hydrogen hydrates we can say that the structural integrity of 216 hydrogen loaded (black line) and 648 hydrogen loaded (blue line) hydrates are the same whereas the second and third peaks of 432 hydrogen loaded hydrate (red line) becomes a bit broad which indicates a little distortion of the clathrate cage.

Analysis of Figs. 4 and 5 leads to the same conclusion that the structural integrity of 432 hydrogen loaded hydrogen hydrate is a bit distorted.
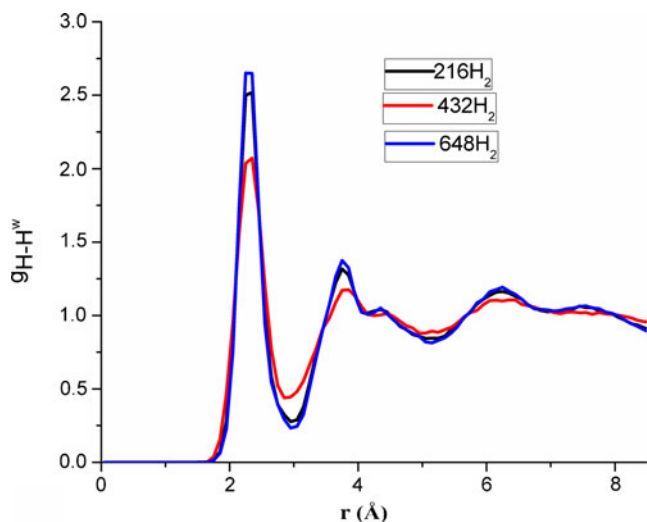

Fig. 5 The H (water)-H (water) radial distribution functions for multiply occupied cages. *Black line* indicates the 216 H_2 molecule encapsulated sI hydrogen hydrate whereas *red* and *blue* indicates those with 432 and 648 H_2 molecules respectively
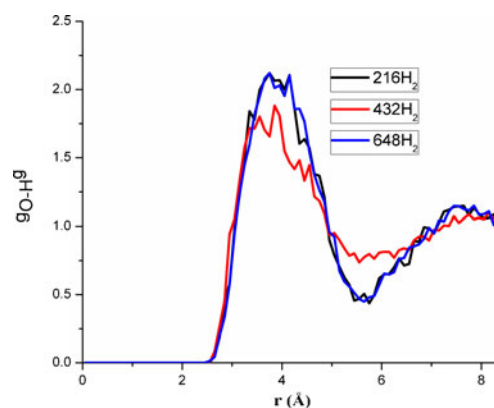

Fig. 6 The O-H (guest) radial distribution functions for multiple occupied cages. *Black line* indicates the 216 H_2 molecule encapsulated sI hydrogen hydrate whereas *red* and *blue* indicates those with 432 and 648 H_2 molecules respectively

Analysis of O-H^g RDF (Fig. 6) gives the first peak at 3.6 Å for 432 hydrogen loaded hydrogen hydrate and at 3.9 Å for 216 as well as 648 hydrogen loaded hydrate. This behavior of water near a hydrophobic solute (hydrogen) does not match with that reported in reference [44] which albeit was not in clathrate hydrates. In the presence of a hydrophobic solute like hydrogen, water molecules push themselves away from hydrogen as well as try to achieve a maximum hydrogen bonded environment [45]. Thus in this case the hydrogen spheres of 432 hydrogen loaded hydrogen hydrate are on an average closer to the oxygen of water than that of the 216 and 648 hydrogen loaded hydrogen hydrates. This orientation leads to a net negative electrostatic potential at the hydrogen center. Coating by methane can reduce the leakage of H_2 through the hexagonal cages in the sI clathrate hydrate [46]. Simulations involving a better electrostatic model to generate a finite quadrupole moment in H_2, e.g., a three-center charge model [44] are being explored.
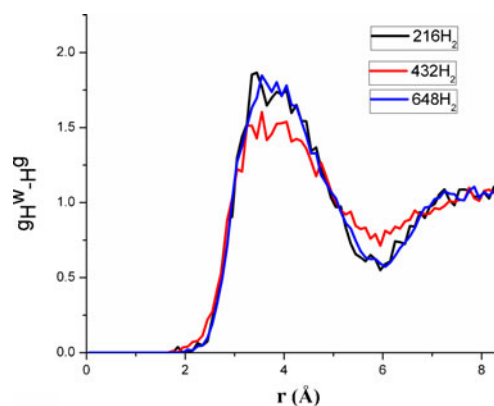

Fig. 7 The H (water)-H (guest) radial distribution functions for multiply occupied cages. *Black line* indicates the 216 H_2 molecule encapsulated sI hydrogen hydrate whereas *red* and *blue* indicates those with 432 and 648 H_2 molecules respectively

The RDF of H^w-H^g is given in Fig. 7. A comparison between O-H^g and H^w-H^g RDF indicates that at a distance of 1.7–2.5 Å the H^w-H^g RDF contains a tail. Appearance of this tail was also reported in reference [44] and it indicates that water hydrogens are closer to the guest hydrogen than that of water oxygen.

A 50 % occupation of the $5^{12}6^2$ clathrate channels where each unit cage contains single H_2 molecule, gives us only 0.72 gravimetric weight percent of hydrogen storage. Now as the number of hydrogen sphere increases in the clathrate slab the binding energy per hydrogen molecule increases. Thus accordingly when the clathrate channels are 100 % occupied where each $5^{12}6^2$ cage contains only one H_2 molecule the binding energy will increase and the gravimetric hydrogen storage will be 1.43 wt.% which albeit is lower than the limit set by DOE [1]. However, when both the 5^{12} and $5^{12}6^2$ cages of the clathrate slab are occupied by more than one hydrogen sphere in each cage then the gravimetric weight percent of hydrogen storage will increase substantially. For any change of the external physical condition the hydrogen hydrate will decompose and liberate hydrogen as a gas spontaneously with water or its vapor depending on the external temperature and pressure conditions as the by-product which is also environment friendly.

Conclusions

From the study of the radial distribution functions of hydrogen loaded hydrates, it is clear that within the simulated time scale the hydrogen hydrate cage is not ruptured.

The interaction energy of hydrogen loading in $5^{12}6^2$ channels of sI clathrate hydrate is negative up to 50 % occupation of the $5^{12}6^2$ cages. Thus the modeled hydrogen hydrate is metastable and may serve the purpose of hydrogen storage.

References

1. www.eere.energy.gov. Accessed 6 April 2012
2. Davy H (1811) Philos Trans R Soc Lond 101:1
3. Faraday M (1823) Philos Trans R Soc Lond 113:60
4. Clausen WF (1951) Suggested structures of water in inert gas hydrates. J Chem Phys 19:259–260
5. Clausen WF (1951) A second water structure for inert gas hydrates. J Chem Phys 19:1425–1426
6. Muller HR, Stackelberg VM (1952) On the structure of gas hydrates- 2 message. Naturwissenschaften 39:20–21
7. Mao W, Mao H, Goncharov A, Struzhkin VV, Guo Q, Hu J, Shu J, Hem-ley R, Somayazulu M, Zhaoi Y (2002) Hydrogen clusters in clathrate hydrate. Science 297:2247–2249
8. Mao WL, Mao HK (2004) Hydrogen storage in molecular compounds. Proc Natl Acad Sci 101:708–710
9. Vos WL, Finger LW, Hemley RJ, Mao HK (1994) Novel H_2-H_2O clathrates at high pressures. Phys Rev Lett 71:3150–3153
10. Powell HM (1948) The structure of molecular compounds. Part IV. Clathrate Compounds. J Chem Soc 61–73 doi:10.1039/JR9480000061
11. Davidson DW, Frank FE (1973) Water: a comprehensive treatise. Plenum Press New York
12. Hammerschmidt EG (1934) Formation of gas hydrates in natural gas transmission lines. Ind Eng Chem 26:851–855
13. Deaton WM, Frost EM (1964) Gas hydrates and their relation to the operation of natural gas pipelines. J U S Bur Mines Monogr 8
14. Waals JH, Platteeuw JC (1959) Clathrate solutions. Adv Chem Phys 2:1–57
15. Somayazulu MS, Finger LW, Hemley RJ, Mao HK (1996) High-pressure compounds in methane-hydrogen mixtures. Science 271:1400–1402
16. Loubeyre P, Letoullec R, Pinceaux JP (1994) Compression of Ar $(H_2)_2$ up to 175 GPa: a new path for the dissociation of molecular hydrogen? Phys Rev Lett 72:1360–1363
17. Lokshin KA, Zhao Y, He D, Mao WL, Mao HK, Hemley RJ, Lobanov MV, Greenblatt M (2004) Structure and dynamics of hydrogen molecules in the novel clathrate hydrate by high pressure neutron diffraction. Phys Rev Lett 93:125503–125506
18. Mao W, Mao HK (2002) Composition and method for hydrogen storage. USA Patent 6735960
19. Stackelberg vM (1949) Solid gas hydrate. Naturwissenschaften 3:327–359
20. Patchkovskii S, Tse J (2003) Thermodynamic stability of hydrogen clathrates. Proc Natl Acad Sci U S A 100:14645–14650
21. Sluiter MF, Adachi H, Belosludov RV, Belosludov V, Kawazoe Y (2004) Ab initio study of hydrogen storage in hydrogen clathrate hydrates. Mater Trans 45:1452–1454
22. Alavi S, Ripmeester JA, Klug DD (2005) Molecular-dynamics study of structure II hydrogen clathrates. J Chem Phys 123:024507–024513
23. Inerbaev TM, Belosludov VR, Belosludov RV, Sluiter M, Kawazoe Y (2006) Dynamics and equation of state of hydrogen clathrate hydrate as a function of cage occupation. Comput Mater Sci 36:229–233
24. Chattaraj PK, Bandaru S, Mondal S (2011) Hydrogen storage in clathrate hydrates. J Phys Chem A 115:187–193
25. Pauling L, Marsh RE (1952) The structure of chlorine hydrate. Proc Natl Acad Sci U S A 38:112–118
26. Jefery GA, Macnicol DD, Bishop R (1996) Solid-state supramolecular chemistry: crystal engineering. In: Comprehensive Supramolecular Chemistry vol 6. Elsevier, Dordrecht, the Netherlands
27. Ripmeester JA, Tse JS, Ratcliffe C, Powell BM (1987) A new clathrate hydrate structure. Nature 325:135–136
28. Udachin KA, Ratcliffe CI, Enright GD, Ripmeester JA (1997) Structure H hydrate: a single crystal diffraction study of 2,2-dimethylpentane center dot 5(Xe, H2S) center dot 34 H2. Supramol Chem 8:173–176
29. Atwood J, Davies JED, Macnicol DD (1991) Inclusion compounds. Oxford University Press, Oxford
30. Sloan ED (2003) Fundamental principles and applications of natural gas hydrates. Nature 426:353–363
31. Liam CJ, Waldemar H, Valeria M (2010) Nucleation pathways of clathrate hydrates: effect of guest size and solubility. J Phys Chem B 114:13796–13807

32. Grigory SS, Vladimir VS (2012) Melting and superheating of sI methane hydrate: molecular dynamics study. J Chem Phys 136:044523–044527
33. Chialvo AA, Mohammed H, Cummings PT (2002) Molecular dynamics study of the structure and thermo physical properties of model sI clathrate hydrates. J Phys Chem B 106:442–451
34. Plimpton SJ (1995) Fast parallel algorithms for short-range molecular dynamics. J Comput Phys 117:1–19
35. Teleman O, Jonsson B, Engstrom S (1987) A molecular dynamics simulation of a water model with intramolecular degrees of freedom. Mol Phys 60:193–203
36. Mizan TI, Savage PE, Ziff RM (1994) Molecular dynamics of supercritical water using a flexible SPC model. J Phys Chem 98:13067–13076
37. Klauda JB, Sandler SI (2003) Phase behavior of clathrate hydrates: a model for single and multiple gas component hydrates. Chem Eng Sci 58:27–41
38. Hirschfelder JO, Curtiss CF, Bird RB (1954) Molecular theory of gases and liquids. Wiley, New York
39. Allen MP, Tildesley DJ (1996) Computer simulation of liquids. Oxford University Press, Oxford
40. Liam CJ, Waldemar H, Valeria M (2009) Thermodynamic stability and growth of guest-free clathrate hydrates: a low-density crystal phase of water. J Phys Chem B 113:10298–10307
41. Valeria M, Moore EB (2009) Water modelled as an intermediate element between carbon and silicon. J Phys Chem B 113:4008–4016
42. Humphrey W, Dalke A, Schulten K (1996) VMD - visual molecular dynamics. J Mol Graph 14:33–38
43. Pratt LR (2002) Molecular theory of hydrophobic effects: "She is too mean to have her name repeated". Annu Rev Phys Chem 53:409–436
44. Sabo D, Rempe SB, Greathouse JA, Martin MG (2006) Molecular studies of the structural properties of hydrogen gas in bulk water. Mol Simul 32(3–4):269–278
45. Stillinger FH (1980) Water revisited. Science 209:451–457
46. Willow SY, Xantheas SS (2012) Chem Phys Lett 525–526:13–18